

Radii and Binding Energies in Oxygen Isotopes: A Challenge for Nuclear Forces

V. Lapoux, V. Somà, C. Barbieri, H. Hergert, J. d. Holt, S. r. Stroberg

▶ **To cite this version:**

V. Lapoux, V. Somà, C. Barbieri, H. Hergert, J. d. Holt, et al.. Radii and Binding Energies in Oxygen Isotopes: A Challenge for Nuclear Forces. Physical Review Letters, 2016, 117 (5), pp.052501. 10.1103/PhysRevLett.117.052501 . cea-01504955

HAL Id: cea-01504955

https://cea.hal.science/cea-01504955

Submitted on 10 Apr 2017

HAL is a multi-disciplinary open access archive for the deposit and dissemination of scientific research documents, whether they are published or not. The documents may come from teaching and research institutions in France or abroad, or from public or private research centers.

L'archive ouverte pluridisciplinaire **HAL**, est destinée au dépôt et à la diffusion de documents scientifiques de niveau recherche, publiés ou non, émanant des établissements d'enseignement et de recherche français ou étrangers, des laboratoires publics ou privés.

Radii and Binding Energies in Oxygen Isotopes: A Challenge for Nuclear Forces

V. Lapoux,[1,*] V. Somà,[1] C. Barbieri,[2] H. Hergert,[3] J. D. Holt,[4] and S. R. Stroberg[4]
[1]CEA, Centre de Saclay, IRFU, Service de Physique Nucléaire, 91191 Gif-sur-Yvette, France
[2]Department of Physics, University of Surrey, Guildford GU2 7XH, United Kingdom
[3]National Superconducting Cyclotron Laboratory and Department of Physics and Astronomy, Michigan State University, East Lansing, Michigan 48824, USA
[4]TRIUMF, 4004 Wesbrook Mall, Vancouver, British Columbia, Canada V6T 2A3
(Received 29 April 2016; published 27 July 2016)

We present a systematic study of both nuclear radii and binding energies in (even) oxygen isotopes from the valley of stability to the neutron drip line. Both charge and matter radii are compared to state-of-the-art *ab initio* calculations along with binding energy systematics. Experimental matter radii are obtained through a complete evaluation of the available elastic proton scattering data of oxygen isotopes. We show that, in spite of a good reproduction of binding energies, *ab initio* calculations with conventional nuclear interactions derived within chiral effective field theory fail to provide a realistic description of charge and matter radii. A novel version of two- and three-nucleon forces leads to considerable improvement of the simultaneous description of the three observables for stable isotopes but shows deficiencies for the most neutron-rich systems. Thus, crucial challenges related to the development of nuclear interactions remain.

DOI: 10.1103/PhysRevLett.117.052501

Our present understanding of atomic nuclei faces the following major questions. Experimentally, we aim (i) to determine the location of the proton and neutron drip lines [1,2], i.e., the limits in neutron numbers N upon which, for fixed proton number Z, with decreasing or increasing N, nuclei are not bound with respect to particle emission, and (ii) to measure nuclear structure observables offering systematic tests of microscopic models. While nuclear masses have been experimentally determined for the majority of known light and medium-mass nuclei [3], measurements of charge and matter radii are typically more challenging. Charge radii for stable isotopes have been accessed in the past by means of electron scattering [4]. In recent years, laser spectroscopy experiments allow extending such measurements to unstable nuclei with lifetimes down to a few milliseconds [5]. Matter radii are determined by scattering with hadronic probes which requires a modelization of the reaction mechanism. Theoretically, intensive works have also been performed towards linking a universal description of atomic nuclei to elementary interactions [6–8] amongst constituent nucleons and, ultimately, to the underlying theory of strong interactions, quantum chromodynamics (QCD). If accomplished, this *ab initio* description would be beneficial both for a deep understanding of known nuclei (stable and unstable, totalling around 3300) and to predict on reliable bases the features of undiscovered ones (few more thousands are expected). Many of the latter are not, in the foreseeable future, experimentally at reach, yet they are crucial to understanding nucleosynthesis phenomena, modelled using large sets of evaluated data and of calculated observables.

The reliability of first-principles calculations depends upon a consistent understanding of fundamental observables: ground-state characteristics of nuclei related to their existence (masses, expressed as binding energies) and sizes (expressed as root mean square—rms—radii). Special interest resides in the study of masses and sizes for a given element along isotopic chains. Experimentally, their determination is increasingly difficult as one approaches the neutron drip line; as of today, the heaviest element with available data on all existing bound isotopes is oxygen ($Z = 8$) [3]. Using theoretical simulations, the link between nuclear properties and internucleon forces can be explored for different N/Z values, thus, critically testing both our knowledge of nuclear forces and many-body theories.

In this work, we focus on oxygen isotopes for which, in spite of the tremendous progress of recent *ab initio* methods, a simultaneous reproduction of masses and radii has not yet been achieved. We present important findings from novel *ab initio* calculations along with a complete evaluation of matter radii, r_m, for stable and neutron-rich oxygen isotopes. Here, r_m are deduced via a microscopic reanalysis of proton elastic scattering data sets. They complement charge radii r_{ch}, offering an extended comparison through the isotopic chain that allows testing state-of-the-art many-body calculations. We show that a recent version of two- and three-nucleon ($2N$ and $3N$) forces leads to considerable improvement in the critical description of radii.

A viable *ab initio* strategy consists in exploiting the separation of scales between QCD and (low-energy) nuclear dynamics, taking point nucleons as degrees of freedom. For decades, realistic $2N$ interactions were built from fitting scattering data, see, e.g., [6]. However, model limitations were seen through discrepancies with experimental data, like underbinding of finite nuclei and inadequate saturation properties of extended nuclear matter.

 © 2016 American Physical Society

More recently, the approach consisted in using the principles of chiral effective field theory (EFT) to provide a systematic construction of nuclear forces, a well-founded starting point for structure calculations [7,8]. Many-body techniques have, themselves, undergone major progress and extended their domain of applicability both in mass and in terms of accessible (open-shell) isotopes for a given element [9–20]. An emblematic case that has received considerable attention is oxygen binding energies, where several calculations have established the crucial role played by $3N$ forces in the reproduction of the neutron drip line at ^{24}O [10,21–26]. The excellent agreement between experimental data and calculations based on a next-to-next-to-next-to-leading order $2N$ and NNLO $3N$ chiral interaction by Entem, Machleidt and others (EM) [27–29] was greeted as a milestone for *ab initio* methods, even though a consistent description of nuclear radii could not be achieved at the same time [30]. Since then, this deficiency has remained a puzzle. Subsequent calculations of heavier systems [11–13] and infinite nuclear matter [31,32] confirmed the systematic underestimation of charge radii, a sizable overbinding and too spread-out spectra, all pointing to an incorrect reproduction of the saturation properties of nuclear matter. While interactions with good saturation properties existed [33–35], this problem led to the focused development of a novel nuclear interaction, NNLO$_{\rm sat}$ [36], which includes contributions up to NNLO in the chiral EFT expansion (both in the $2N$ and $3N$ sectors) and differs from EM in two main aspects. First, the optimization of the ("low-energy") coupling constants is performed simultaneously for $2N$ and $3N$ terms [37]; EM, in contrast, optimizes $3N$ forces subsequently. Second, in addition to observables from few-body ($A = 2$, 3, 4) systems, experimental constraints from light nuclei (energies and charge radii in some C and O isotopes) are included in the optimization. This aspect departs from the strategy of EM, in which parameters in the A-body sector are fixed uniquely by observables in A-body systems. Although first applications point to good predictive power for ground-state properties [36,38,39], the performance of the NNLO$_{\rm sat}$ potential remains to be tested along complete isotopic chains.

Here, we employ two different many-body approaches, self-consistent Green's function (SCGF) and in-medium similarity renormalization group (IMSRG), each available in two versions. The first are based on standard expansion schemes and, thus, are applicable only to closed-shell nuclei (e.g., not ^{18,20}O): Dyson SCGF (DGF) [40] and single-reference IMSRG (SR-IMSRG) [41], respectively. The second are built on Bogoliubov-type reference states and, thus, allow for a proper treatment of pairing correlations and systems displaying an open-shell character. These are labeled Gorkov SCGF (GGF) [9] and multireference IMSRG (MR-IMSRG) [10], respectively. For the MR-IMSRG, the reference state is first projected on good proton and neutron numbers. Having different *ab initio* approaches at hand is crucial for benchmarking theoretical results and inferring as unbiased as possible information on the input forces. Moreover, while DGF, SR-IMSRG, and MR-IMSRG feature a comparable content in terms of many-body expansion, GGF currently includes a lower amount of many-body correlations, which allows testing the many-body convergence [11].

First, we compute binding energies E_B for $^{14-24}$O for the two sets of $2N$ and $3N$ interactions with the four many-body schemes. EM is further evolved to a low-momentum scale $\lambda = 1.88$–2.0 fm^{-1} by means of SRG techniques [42,43]. Results are displayed in Fig. 1. For both interactions, different many-body calculations yield values of E_B spanning intervals of up to 10 MeV, from 5% to 10% of the total. Compared to experimental binding energies, EM and NNLO$_{\rm sat}$ perform similarly, following the trend of available data along the chain both in absolute and in relative terms. Overall, results shown in Fig. 1 confirm previous findings for EM and validate the use along the isotopic chain for NNLO$_{\rm sat}$.

Now, we examine the nuclear charge observables. In addition to $r_{\rm ch}$ radii, analytical forms of fitted experimental charge densities can be extracted from (e, e) cross sections. Standard forms include two-parameter or three-parameter Fermi (2PF or 3PF) profiles [44]. By unfolding [45] the finite size of proton charge distribution [whose $r_{\rm ch}$ radius is 0.877(7) fm [46]], proton ground-state densities ρ_p can be deduced, and the corresponding r_p radius defined as the rms radius of the $\rho_p(r)$ distribution ($\sqrt{\langle r^2 \rangle}$). It should be underlined that, due to the various analysis techniques providing charge densities, the global systematic error on r_p is significantly larger (roughly 0.05 fm) than the one on single $r_{\rm ch}$ values (of the order of 0.01 fm). For ^{16}O, $r_{\rm ch}$ was estimated to be 2.730 (25) fm [47] and 2.737 (8) fm [44,48]. Differences in $r_{\rm ch}$ between ^{17,18}O and ^{16}O, $\Delta r_{\rm ch} = -0.008(7)$ and $+0.074(8)$ fm [48], are affected by the same systematic errors.

In this Letter, we determine matter radii via the proton probe. We consider angular distributions of proton elastic

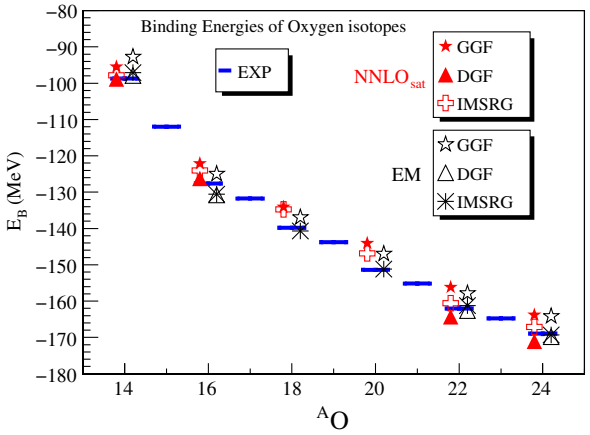


FIG. 1. Oxygen binding energies. Results from SCGF (DGF and GGF) and IMSRG calculations with EM and NNLO$_{\rm sat}$ are displayed along with experimental data.

scattering cross sections and compare data to calculations performed using a microscopic density-dependent optical model potential (OMP) inserted in the distorted wave Born approximation. Recently, this type of analysis has been successfully applied to the case of helium isotopes, for which r_m radii were extracted with uncertainties of the order of 0.1 fm [49]. We employ the energy- and density-dependent Jeukenne-Lejeune-Mahaux (JLM) potential [50], derived from a G-matrix formalism and extensively tested in the analysis of nucleon scattering data for a wide range of nuclei. This complex potential depends only on the incident energy E and on neutron and proton densities. Here, we use the standard form:

$$U_{\mathrm{JLM}}(\rho, E) = \lambda_V V(\rho, E) + i\lambda_W W(\rho, E),$$

with $\lambda_V = \lambda_W = 1$.

For $^{18-22}$O, nucleon separation energies are sufficiently high to exclude strong coupling effects to continuum or to excited states, and the imaginary part is enough to include, implicitly, all other relevant coupled-channel effects.

For the stable symmetric ^{16}O, r_m was extracted from combined (e, e), (p, p), and (n, n) in Ref. [51] using the following procedure: the (3PF) density profile ρ_p was deduced from electron scattering data [47], the same profile was assumed for the neutron density distribution. This "experimental" matter density built from the (e, e) data was used to compute the potentials. This procedure was also followed for ^{17,18}O, with the neutron density profiles initially taken as $(N/Z) * \rho_p$ then adjusted to reproduce elastic data on heavy ions [45]. We refer to densities extracted in this way as the experimental (exp) ones, with r_p values for $^{16-18}$O given in Table I.

We first performed OMP calculations for ^{18}O and compared them to data collected at 35.2 $A \cdot$ MeV in direct kinematics [54] and at 43 $A \cdot$ MeV in inverse kinematics [55]. Starting from a 2PF profile fitted to exp densities, by changing the two parameters governing size and diffusiveness, we generated a family of densities then inserted into the OMP and fitted to data. Since only the most forward angles have small global errors and are sensitive to the size of the nucleus, we limited our fit to 46° and 33° for 35.2 and 43 $A \cdot$ MeV data, respectively, i.e., to data with statistical + systematic errors below 10%. By keeping the curves falling within $\chi^2/\mathrm{d.o.f.} < 1$, we determined an associated matter radius $r_m = 2.75(10)$ fm. The 2PF profiles with the same r_m lead to very similar $\chi^2/\mathrm{d.o.f.}$, signaling that calculations, in the region of forward angles, are rather insensitive to the diffusiveness. As shown in Fig. 2, calculations are in good agreement with (p, p) data, which confirms the validity of the OMP approach provided that realistic densities are employed. We repeated the analysis using densities generated by Hartree-Fock BCS calculations [55] with Skyrme interactions, each associated with a different r_m. Results are very similar to the ones of Fig. 2, with $r_m = 2.77(10)$ fm, close to the one from exp densities. This validates the use of OMP calculations to estimate r_m radii from (p, p) cross sections [49].

For unstable ^{20,22}O, elastic proton scattering cross sections were measured using oxygen beams at 43 and 46.6 $A \cdot$ MeV, respectively [55,56]. We performed OMP calculations with microscopic densities for ^{20,22}O. Angular distributions up to 30° (for ^{20}O) and 33° (for ^{22}O) were considered for the fits. Results are displayed in Fig. 2. In order to show the sensitivity to the microscopic inputs, we compare, for ^{22}O, results with densities from the Sly4 [57] Skyrme interaction with those obtained with densities from Hartree-Fock-Bogoliubov calculations based on the Gogny D1S force [58,59]. In both cases, (p, p) cross sections are well reproduced. Resulting r_m radii are 2.90 fm in ^{20}O along with 2.96 and 3.03 fm in ^{22}O for Sly4 and D1S densities, respectively. The sensitivity study led us to the same range of ± 0.1 fm, which is the uncertainty on our values throughout the (p, p) analysis. The results are summarized in Table I.

Studying interaction cross sections (σ_I) [53] is another way of deducing matter radii. In Fig. 3, we compare experimental r_m radii for $^{16-22}$O from (e, e) and (p, p)

TABLE I. Experimental rms radii (in fm) of O isotopes: r_p for $^{16-18}$O are extracted from charge densities [44,45,52]. For $A = 16$, r_m is evaluated from (p, p) data [51], and for $A = 17$, via heavy-ion scattering [45]. r_m from σ_I are given in Ref. [53]. For $A =$ 18–22, "r_m (p, p)" values are from the present work and are explained in the text.

A	16	17	18	20	22
r_p	2.59 (7)	2.60 (8)	2.68 (10)		
r_m (σ_I)	2.54 (2)	2.59 (5)	2.61 (8)	2.69(3)	2.88(6)
r_m (p, p)	2.60 (8)	2.67 (10)	2.77 (10)	2.9 (1)	3.0 (1)

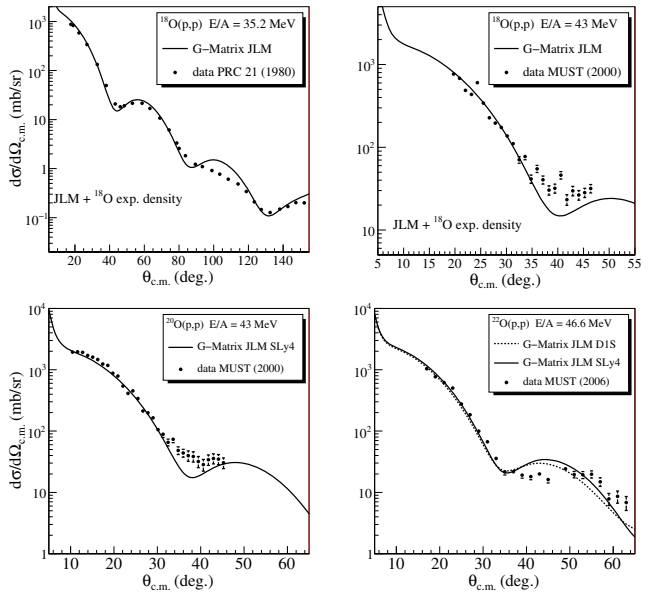


FIG. 2. Experimental elastic (p, p) distributions compared to OMP calculations (this work). (Top) ^{18}O (data: [54,55]). (Bottom) ^{20,22}O (data: [55,56]).

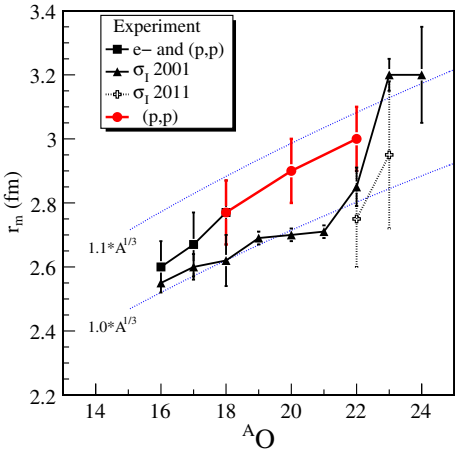


FIG. 3. Experimental values for the r_m radii, deduced from σ_I, (e, e) and (p, p) measurements (see Table I). Blue lines show the $A^{1/3}$ behavior of the liquid drop model.

to values obtained from σ_I measurements [53,60] (see, also, Table I). While (e, e) and (p, p) provide a consistent set of r_p and r_m radii for $^{16-18}$O, this is not the case for r_m values obtained from σ_I, usually extracted without including correlations in the target, which arguably influences scattering amplitudes. Since our analysis of the stable isotopes, used as a reference, provides r_m radii with an uncertainty of the order of 0.1 fm, we also conclude that uncertainties deduced from σ_I are underestimated. Consequently, we focus on results obtained from (e, e) and (p, p) data for the comparison with theory.

We start by analyzing calculations for proton and neutron radii, shown in Fig. 4. We notice that, for each interaction, there is good agreement between the various methods, which span 0.05 (0.1) fm when EM ($NNLO_{sat}$) is used. This shows that different state-of-the-art schemes achieve, for a given interaction, an uncertainty that is smaller than (i) experimental uncertainty and (ii) the uncertainty coming from the use of different interactions. Clear discrepancies are observed between radii computed with EM and $NNLO_{sat}$, with the former being systematically smaller by 0.2–0.3 fm. While EM largely underestimates data, r_p values are well reproduced by $NNLO_{sat}$, keeping in mind that r_{ch} of ^{16}O is included in the $NNLO_{sat}$ fit. The performance of the interactions along the isotopic chain can be seen for matter radii, where, in Fig. 5, the evaluations from the (p, p) analysis are compared to GGF and MR-IMSRG. Similar conclusions are drawn by considering other schemes, e.g., see Fig. 4, where rms radii computed with EM underestimate evaluated data by about 0.3–0.4 fm for all isotopes. Results significantly improve with $NNLO_{sat}$, although the description deteriorates towards the neutron drip line, with a discrepancy of about 0.2 fm in ^{22}O. Recently, a similar effect was observed for the calcium isotopes [39].

These results reinforce the progress of nuclear *ab initio* calculations, which are able to address systematics of isotopic chains beyond light systems and, thus, provide

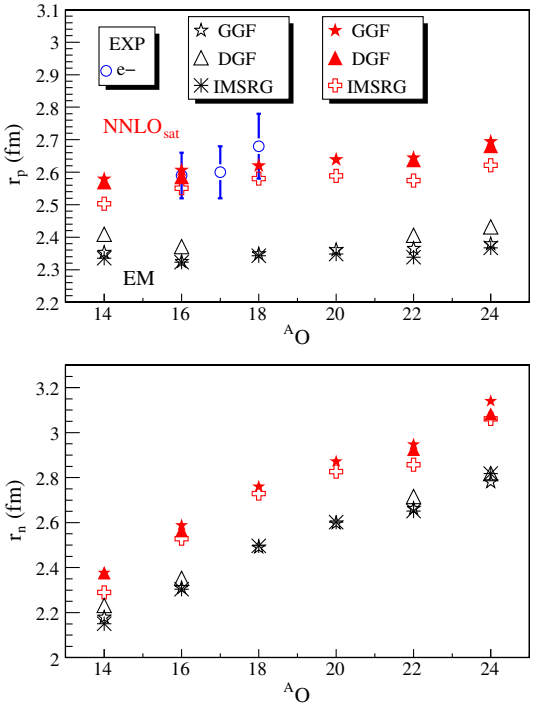


FIG. 4. Proton (top) and neutron (bottom) radii obtained from IMSRG and SCGF calculations with EM and $NNLO_{sat}$. Experimental r_p values are given in Table I.

critical feedback on the long-term developments of internucleon interactions. To this extent, joint theory-experiment analyses are essential and have to start with a realistic description of both sizes and masses. In this Letter, we focused on the oxygen chain, the heaviest one for which experimental information on both E_B and radii is available up to the neutron drip line. We showed that nuclear sizes of unstable isotopes can be obtained through the (p, p) data analysis within 0.1 fm. The combined comparison of measured charge-matter radii and E_B with

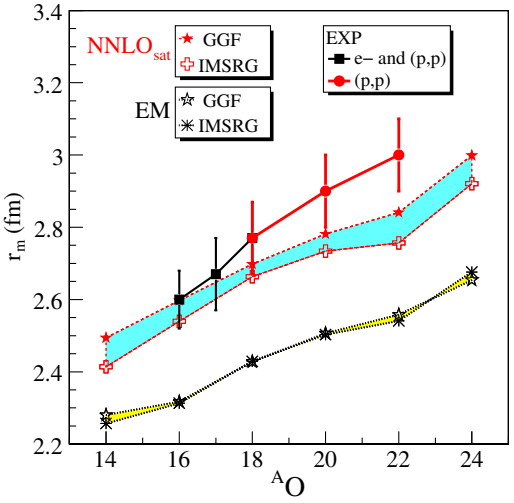


FIG. 5. Matter radii from our analysis and given in Table I, compared to calculations with EM [27–29] and $NNLO_{sat}$ [36]. Bands span results from GGF and MR-IMSRG schemes.

ab initio calculations offers a unique insight on nuclear forces: the current standard EM yields an excellent reproduction of E_B but significantly underestimates radii, whereas the unconventional $\mathrm{NNLO_{sat}}$ clearly improves the description of radii. Our results raise questions about the choice of observables that should be included in the fit and the resulting predictive power whenever this strategy is followed.

More precise information on oxygen radii, e.g., r_{ch} via laser spectroscopy measurements, would allow confirming our (p, p) analysis and further refining the present discussion. Similar studies in heavier isotopes will also contribute to the systematic development of nuclear forces. Finally, we stress that a simultaneous reproduction of binding energies and radii in stable and neutron-rich nuclei is mandatory for reliable structure but even more for reaction calculations. Scattering amplitudes and nucleon-nucleus interactions evolve as a function of the size, which should be consistently taken into account when more microscopic reaction approaches are considered.

The Espace de Structure et de réactions Nucléaires Théorique (ESNT) framework at CEA is gratefully acknowledged for supporting the project that initiated the present work. The authors would like to thank T. Duguet for useful discussions and P. Navrátil, A. Calci, S. Binder, J. Langhammer, and R. Roth for providing the interaction matrix elements used in the present calculations. C. B. is funded by the Science and Technology Facilities Council (STFC) under Grant No. ST/L005743/1. SCGF calculations were performed by using HPC resources from GENCI-TGCC (Contracts No. 2015-057392 and No. 2016-057392) and the DiRAC Data Analytic system at the University of Cambridge (under BIS National E-infrastructure capital grant ST/J005673/1 and STFC Grants No. ST/H008586/1 and No. ST/K00333X/1). H. H. acknowledges support by the NSCL/FRIB Laboratory. TRIUMF receives federal funding via a contribution agreement with the National Research Council of Canada. Computing resources for MR-IMSRG calculations were provided by the Ohio Supercomputing Center (OSC) and the National Energy Research Scientific Computing Center (NERSC), a DOE Office of Science User Facility supported by the Office of Science of the U.S. Department of Energy under Contract No. DE-AC02-05CH11231.

*vlapoux@cea.fr

[1] J. Erler, N. Birge, M. Kortelainen, W. Nazarewicz, E. Olsen, A. M. Perhac, and M. Stoitsov, Nature (London) **486**, 509 (2012).
[2] M. Thoennessen, Int. J. Mod. Phys. E **24**, 1530002 (2015).
[3] G. Audi, M. Wang, A. H. Wapstra, F. G. Kondev, M. MacCormick, X. Xu, and B. Pfeiffer, Chin. Phys. C **36**, 1287 (2012).
[4] R. Hofstadter, Rev. Mod. Phys. **28**, 214 (1956).
[5] J. Billowes and P. Campbell, J. Phys. G **21**, 707 (1995).
[6] R. Machleidt and I. Slaus, J. Phys. G **27**, R69 (2001) (topical review), and references therein.
[7] E. Epelbaum, H.-W. Hammer, and U.-G. Meißner, Rev. Mod. Phys. **81**, 1773 (2009).
[8] R. Machleidt and D. Entem, Phys. Rep. **503**, 1 (2011).
[9] V. Somà, T. Duguet, and C. Barbieri, Phys. Rev. C **84**, 064317 (2011).
[10] H. Hergert, S. Binder, A. Calci, J. Langhammer, and R. Roth, Phys. Rev. Lett. **110**, 242501 (2013).
[11] V. Somà, A. Cipollone, C. Barbieri, P. Navrátil, and T. Duguet, Phys. Rev. C **89**, 061301 (2014).
[12] S. Binder, J. Langhammer, A. Calci, and R. Roth, Phys. Lett. B **736**, 119 (2014).
[13] H. Hergert, S. K. Bogner, T. D. Morris, S. Binder, A. Calci, J. Langhammer, and R. Roth, Phys. Rev. C **90**, 041302 (2014).
[14] J. D. Holt, J. Menéndez, and A. Schwenk, Phys. Rev. Lett. **110**, 022502 (2013).
[15] J. D. Holt, J. Menendez, J. Simonis, and A. Schwenk, Phys. Rev. C **90**, 024312 (2014).
[16] G. Hagen, T. Papenbrock, M. Hjorth-Jensen, and D. J. Dean, Rep. Prog. Phys. **77**, 096302 (2014).
[17] S. K. Bogner, H. Hergert, J. D. Holt, A. Schwenk, S. Binder, A. Calci, J. Langhammer, and R. Roth, Phys. Rev. Lett. **113**, 142501 (2014).
[18] G. R. Jansen, J. Engel, G. Hagen, P. Navrátil, and A. Signoracci, Phys. Rev. Lett. **113**, 142502 (2014).
[19] A. Signoracci, T. Duguet, G. Hagen, and G. R. Jansen, Phys. Rev. C **91**, 064320 (2015).
[20] T. Duguet, J. Phys. G **42**, 025107 (2015).
[21] T. Otsuka, T. Suzuki, J. D. Holt, A. Schwenk, and Y. Akaishi, Phys. Rev. Lett. **105**, 032501 (2010).
[22] G. Hagen, M. Hjorth-Jensen, G. R. Jansen, R. Machleidt, and T. Papenbrock, Phys. Rev. Lett. **108**, 242501 (2012).
[23] J. D. Holt, J. Menéndez, and A. Schwenk, Eur. Phys. J. A **49**, 39 (2013).
[24] A. Cipollone, C. Barbieri, and P. Navrátil, Phys. Rev. Lett. **111**, 062501 (2013).
[25] T. A. Lähde, E. Epelbaum, H. Krebs, D. Lee, U.-G. Meißner, and G. Rupak, Phys. Lett. B **732**, 110 (2014).
[26] K. Hebeler, J. D. Holt, J. Menéndez, and A. Schwenk, Annu. Rev. Nucl. Part. Sci. **65**, 457 (2015).
[27] D. R. Entem and R. Machleidt, Phys. Rev. C **68**, 041001 (2003).
[28] P. Navrátil, Few-Body Syst. **41**, 117 (2007).
[29] R. Roth, S. Binder, K. Vobig, A. Calci, J. Langhammer, and P. Navrátil, Phys. Rev. Lett. **109**, 052501 (2012).
[30] A. Cipollone, C. Barbieri, and P. Navrátil, Phys. Rev. C **92**, 014306 (2015).
[31] A. Carbone, A. Polls, and A. Rios, Phys. Rev. C **88**, 044302 (2013).
[32] G. Hagen, T. Papenbrock, A. Ekström, K. A. Wendt, G. Baardsen, S. Gandolfi, M. Hjorth-Jensen, and C. J. Horowitz, Phys. Rev. C **89**, 014319 (2014).
[33] K. Hebeler, S. K. Bogner, R. J. Furnstahl, A. Nogga, and A. Schwenk, Phys. Rev. C **83**, 031301(R) (2011).
[34] L. Coraggio, J. W. Holt, N. Itaco, R. Machleidt, L. E. Marcucci, and F. Sammarruca, Phys. Rev. C **89**, 044321 (2014).
[35] J. Simonis, K. Hebeler, J. D. Holt, J. Menéndez, and A. Schwenk, Phys. Rev. C **93**, 011302(R) (2016).

[36] A. Ekström, G. R. Jansen, K. A. Wendt, G. Hagen, T. Papenbrock, B. D. Carlsson, C. Forssén, M. Hjorth-Jensen, P. Navrátil, and W. Nazarewicz, Phys. Rev. C **91**, 051301 (2015).
[37] B. D. Carlsson, A. Ekström, C. Forssén, D. F. Strömberg, G. R. Jansen, O. Lilja, M. Lindby, B. A. Mattsson, and K. A. Wendt, Phys. Rev. X **6**, 011019 (2016).
[38] G. Hagen *et al.*, Nat. Phys. **12**, 186 (2015).
[39] R. F. Garcia Ruiz *et al.*, Nat. Phys. **12**, 594 (2016).
[40] W. H. Dickhoff and C. Barbieri, Prog. Part. Nucl. Phys. **52**, 377 (2004).
[41] K. Tsukiyama, S. K. Bogner, and A. Schwenk, Phys. Rev. Lett. **106**, 222502 (2011).
[42] S. K. Bogner, R. J. Furnstahl, and R. J. Perry, Phys. Rev. C **75**, 061001(R) (2007).
[43] S. K. Bogner, R. J. Furnstahl, and A. Schwenk, Prog. Part. Nucl. Phys. **65**, 94 (2010).
[44] H. De Vries, C. W. De Jager, and C. De Vries, At. Data Nucl. Data Tables **36**, 495 (1987), and references therein.
[45] G. R. Satchler and W. G. Love, Phys. Rep. **55**, 183 (1979).
[46] K. Nakamura *et al.* (Particle Data Group), J. Phys. G **37**, 075021 (2010).
[47] I. Sick and J. S. McCarthy, Nucl. Phys. **A150**, 631 (1970).
[48] H. Miska, B. Norum, M. V. Hynes, W. Bertozzi, S. Kowalski, F. N. Rad, C. P. Sargent, T. Sasanuma, and B. L. Berman, Phys. Lett. **83B**, 165 (1979).
[49] V. Lapoux and N. Alamanos, Eur. Phys. J. A **51**, 91 (2015).
[50] J. P. Jeukenne, A. Lejeune, and C. Mahaux, Phys. Rev. C **16**, 80 (1977).
[51] J. S. Petler, M. S. Islam, R. W. Finlay, and F. S. Dietrich, Phys. Rev. C **32**, 673 (1985).
[52] B. Norum *et al.*, Phys. Rev. C **25**, 1778 (1982).
[53] A. Ozawa, T. Suzuki, and I. Tanihata, Nucl. Phys. **A693**, 32 (2001).
[54] E. Fabrici, S. Micheletti, M. Pignanelli, F. G. Resmini, R. De Leo, G. D'Erasmo, and A. Pantaleo, Phys. Rev. C **21**, 844 (1980).
[55] E. Khan *et al.*, Phys. Lett. B **490**, 45 (2000).
[56] E. Becheva *et al.* (MUST Collaboration), Phys. Rev. Lett. **96**, 012501 (2006).
[57] E. Chabanat, P Bonche, P. Haensel, J. Meyer, and R. Schaeffer, Nucl. Phys. **A635**, 231 (1998).
[58] J. Dechargé and D. Gogny, Phys. Rev. C **21**, 1568 (1980).
[59] J.-F. Berger, M. Girod, and G. Gogny, Comput. Phys. Commun. **63**, 365 (1991).
[60] R. Kanungo *et al.*, Phys. Rev. C **84**, 061304(R) (2011).